HYDROGEN DISPERSION FOLLOWING BLOWDOWN RELEASES INTO A TUNNEL

Lyons, K.[1], Rattigan, W. [1], Moodie, K. [1], Ewan, B., Fletcher, J. [1] and Atkinson, G. [1]
[1] Major Hazards, Science Division, Health and Safety Executive, Harpur Hill, Buxton, Derbyshire, SK17 9DZ, UK
Kieran.Lyons@hse.gov.uk; Wayne.Rattigan@hse.gov.uk; James.Fletcher@hse.gov.uk

ABSTRACT

This paper presents work undertaken by the HSE as part of the Hytunnel-CS project, a consortium investigating safety considerations for fuel cell hydrogen (FCH) vehicles in tunnels and similar confined spaces. The test programme investigating hydrogen dispersion in tunnels involved simulating releases analogous to Thermally activated Pressure Relief Devices (TPRDs), typically found on hydrogen vehicles, into the HSE Tunnel facility. The releases were scaled and based upon four scenarios: cars, buses, and two different train designs. The basis for this scaling was the size of the tunnel and the expected initial mass flow rates of the releases scenarios. The results of the 12 tests completed have been analysed in two ways: the initial mass flow rates of the tests were calculated based upon facility measurements and the Able-Noble equations of state for comparison to the intended initial flow rate; and observations of the hydrogen dispersion in the tunnel were made based on 15 hydrogen sensors arrayed along the tunnel. The calculated mass flow rates showed reasonable agreement with the intended initial conditions, showing that the scaling methodology can be used to interpret the data based on the full-scale tunnel of interest. Observations of the hydrogen dispersion show an initial turbulent mixing followed by a movement of the mixed hydrogen/air cloud down the tunnel. No vertical stratification of the cloud was observed but this effect could be possible in longer tunnels or tunnels with larger diameters. Higher ventilation rates in the tunnel resulted in a reduction of the residence time of the hydrogen and a slight increase in the dilution.

1.0 INTRODUCTION

1.1 Project Background

The HyTunnel project [1] is a large project conducted by an international consortium. The objective was to investigate the safety implications of hydrogen vehicles (compressed hydrogen storage) entering confined spaces such as tunnels and garages prior to large-scale adoption of the technology [2]. Various theoretical and practical studies were undertaken to this end, including a series of dispersion experiments carried out by HSE [3].

1.2 Experimental Objectives

The main objective of this series of experiments was to generate hydrogen dispersion data for realistic (scaled) hydrogen releases in a tunnel. The releases for this section would simulate a thermally activated pressure relief device (TPRD) in operation on hydrogen vehicles. This required source term definition as well as hydrogen concentration measurements throughout the tunnel. Two levels of ventilation were used to explore the dispersion with various flow conditions. The data generated will be used to validate hydrogen dispersion models, which will then be used to predict the total flammable extent for realistic accident and release scenarios [4] [5].

To meet this objective, a series of 12 experiments were carried out whereby a vessel was pressurised through a series of booster pumps to the scaled pressure, then hydrogen was released through a nozzle. This scaling was based on equivalent initial mass flow rates for the defined scenarios. Four scaled scenarios were investigated: Car, Bus, Train 1, and Train 2. These were each tested with two

ventilation rates. The experimental outputs are pipework measurements to define the hydrogen source, and concentration measurements down the tunnel to measure the dispersion.

2.0 METHODS

2.1 Experimental Facility

The HyTunnel facility at the HSE science and Research Centre has five main components: the large, steel tunnel; the gas delivery rig; the fan structure for providing the ventilation; the experimental delivery method; and the experimental sensors.

The tunnel is 70 m long, 3.7 m diameter and the hydrogen was released in the centre. Figure 2 shows a sketch of the tunnel, taken as a cross-section, showing the dimensions for the release points. The tunnel lies flat on the ground longitudinally and is open at both ends. One end had a mobile fan structure and flow-straighteners, which provided the ventilation rates of 1.25 and 2.4 m/s for some of the tests. Test 1, however, was completed with 'natural ventilation', which varied based on the ambient wind conditions but was nominally still.

Figure 1: Image of the tunnel, gas delivery rig (centre) and fan structure (left).

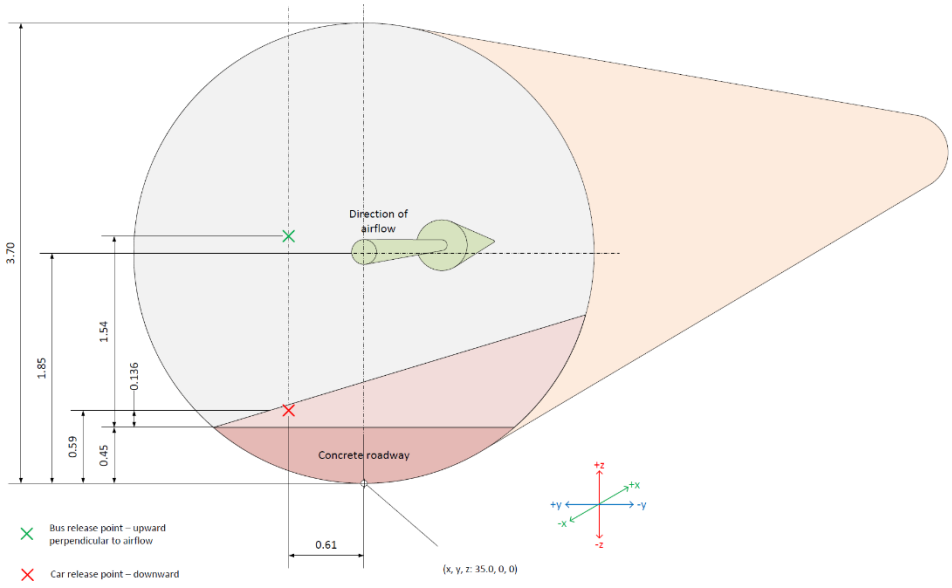

Figure 2: Sketch of the tunnel layout showing release points and dimensions

The hydrogen was boosted from bottle pressure (17 MPa) to test pressure (up to 59 MPa) and stored in the facility prior to the tests. The hydrogen was then released into the centre of the tunnel as a blowdown to simulate the operation of a TPRD. The volume of the storage vessels and associated pipework was 0.0565 m^3 for the car releases, and 0.162 m^3 for the other cases. Table 1 shows the nozzle diameters used and the initial conditions for the four scenarios: car, bus, train 1, train 2.

Table 1: Experimental conditions for each scenario.

Scenario	Nozzle diameter (mm)	Hydrogen volume (m^3)	Storage Pressure (MPa)
Car	2.25	0.0565	11.8
Bus	4.07	0.162	31
Train 1	5.73	0.162	51
Train 2	4.77	0.162	58

Pressure and temperature measurements were taken at the release point to characterise the source term (release parameters). The dispersion of the hydrogen was measured with concentration sensors distributed down the tunnel based on the HyWAM concept [6]. Table 2 shows the ranges and accuracies of these sensors. Table 3 shows the positions of the hydrogen concentration sampling points and the approximate sample delay time. The heights are based on the coordinate system from Figure 2, and a 0.45 m concrete floor in in place. This means that the height *z* of 0.95 m is 0.5 m from the concrete floor of the tunnel. The times are approximate and vary throughout the experimental campaign due to individual pump performance.

Table 2: Sensor accuracies.

Sensor type	Make/model	Range	Accuracy
Pressure transducer	Druck Unik 5800	0-70 MPa (gauge)	± 0.6% FS
Thermocouple	Type K insulated	0-1100 °C	± 0.2 ºC
Hydrogen concentration	XENSOR XEN-5320	0-100 % H_2	± 1% FS

Table 3: Hydrogen concentration sensor locations.

ID	Position	*x* (m)	*y* (m)	*z* (m)	Delay (s)*
02E002	A high	34.0	0.0	3.25	7.3
02E003	B low	37.5	0.0	0.95	11.7
02E004	B mid	37.5	0.0	2.15	5.7
02E005	B high	37.5	0.0	3.25	6.5
02E006	C far	40.0	-1.7	2.15	10.1
02E026	C near	40.0	-1.2	2.15	6.6
02E008	D low	42.5	0.0	0.95	5.8
02E009	D mid	42.5	0.0	2.15	7.0
02E010	D high	42.5	0.0	3.25	6.8
02E011	E far	45.0	-1.7	2.15	11.7
02E012	E near	45.0	-1.2	2.15	12.7
02E013	F low	50.0	0.0	0.95	10.0
02E014	F mid	50.0	0.0	2.15	6.2
02E015	F high	50.0	0.0	3.25	7.1
02E016	H high	60.0	0.0	3.25	6.7

*The uncertainty on the delay time for each sensor is approximately ± 3 s.

2.2 Scaling Methodology

Since the HSE tunnel is smaller compared to a typical road or rail tunnel, scaling has been used to allow for extrapolation of the results. The scaling used is an existing method [7] and discussed in

detail previously [8]. This section shows a summary of the method to enable an application to the results.

The main objective of the scaling is to enable a similar hydrogen concentration at the normalised height of the HSE tunnel, which will be applicable to real tunnels. This is achieved by scaling the hydrogen mass and mass flow rates of real scenarios by a factor based on the relative diameters of the HSE tunnel to a real tunnel. Based on this scaling and practical constraints (hydrogen cylinder volume availability), the initial conditions for the experiments were selected. These factors will be applied to the measured concentrations to describe the real scenario modelled.

The scaling factors are derived as follows and displayed for the HSE scenarios in Table 4:

- Scaling factor (SF) for tunnel diameter is D/D_{HSE}
- Scaling factor for mass of hydrogen stored is SF^3
- Scaling factor for the mass flow rate is $SF^{5/2}$.
- Scaling factor for the discharge time is: $SF^{1/2}$.
- Scaling factor for the airflow in the tunnel is: $SF^{1/2}$.

Table 4: Scaling factors for each scenario.

Scenario	SF	SF (mass)	SF (mass flow rate)	SF (discharge time)	SF (airflow)
Car	2.275	11.775	7.806	1.508	1.508
Bus	2.275	11.775	7.806	1.508	1.508
Train 1	2.665	18.927	11.594	1.632	1.632
Train 2	2.665	18.927	11.594	1.632	1.632

2.3 Pre-trial Simulations

Pre-trial simulations of the blowdowns, specifically regarding the mass flow rates in the storage vessels, were completed as a basis of comparison for the measured blowdown rates. Using the suite of tools available on E-labs [9], the mass of hydrogen against time for adiabatic and isothermal conditions for each scenario were modelled. The flow rates were subsequently compared to the measured values, providing an approximate discharge coefficient, which enables a discussion about the suitability of the experiments to match the intended initial conditions.

2.4 Mass Flow Rate Calculations

With the design intention of achieving relatively high initial mass flow rates, a mass flow meter was not included in the pipework to avoid constrictions. As such, the mass flow rate of each blowdown was calculated rather than directly measured. The method used is described below:

Using a rearrangement of the Able-Noble equations of state, shown in equation 1 [10], the density of the hydrogen was calculated using pressure and temperature measurements made in the facility.

$$\boldsymbol{\rho = \frac{P}{bP + R_{H2}T}} \quad (1)$$

where ρ is the density of hydrogen at time t (kg/m^3), P is the measured pressure in the vessel at time t (Pa), b is the co-volume of hydrogen (m^3/kg), R_{H2} is the gas constant of hydrogen (J/kg K), and T is the measured temperature in the vessel at time t (K).

The mass was then calculated at each time using equation 2.

$$\boldsymbol{m = \rho V} \quad (2)$$

where m is mass of hydrogen in the vessel at time t (kg), ρ is the density of hydrogen at time t (kg/m^3), and V is the volume of the vessel and intrinsic pipework (m^3).

The results of this step give the mass decay curves. From these the mass flow rates can be estimated. This was completed by exponential regression of the initial 10 seconds of the mass decay curves; differentiation then gives an estimate for the mass flow rate. The regression took the form shown in equation 3, with equation 4 being the result of differentiation.

$$\boldsymbol{m \approx f(t) \approx e^{at^2+bt+c}} \quad (3)$$

where m is mass of hydrogen in the vessel at time t (kg), t is the time (s), and a b c are constants obtained through the regression method.

$$\dot{m} \approx \frac{\boldsymbol{df(t)}}{\boldsymbol{dt}} \approx \boldsymbol{-(2at+b)e^{at^2+bt+c}} \quad (4)$$

where m is mass of hydrogen in the vessel at time t (kg), t is the time (s), and a b c are constants obtained through the regression method.

3.0 RESULTS AND DISCUSSION

3.1 Initial conditions

A total of 12 unignited blowdown releases were completed. Test 2 to 12 were completed with the fan system operating, so have a known ventilation rate. The initial conditions for these tests are displayed in Table 5.

Table 5: Experimental series summary conditions and results.

Test No.	Scenario	Initial pressure (MPa)*	Release height (mm)	Release orientation	Wind speed (m/s)	Initial mass (kg)	Initial mass flow rate (kg/s)
1	Car	11.6	137	Downwards	0.2 to 0.7	0.52	0.033
2	Car	11.5	137	Downwards	0.9 to 1.3	0.51	0.035
3	Car	11.6	137	Downwards	2.1 to 2.6	0.51	0.036
4	Bus	30.1	1407	Upwards	0.8 to 1.5	3.36	0.306
5	Bus	30.5	1407	Upwards	2.2 to 2.7	3.43	0.319
6	Train 2	55.5	1407	Upwards	0.8 to 1.5	5.30	0.680
7	Train 2	55.5	1407	Upwards	2.2 to 2.9	5.55	0.751
8	Train 1	49.0	1407	Upwards	1.0 to 1.7	5.04	0.947
9	Train 1	49.6	1407	Upwards	2.2 to 2.8	5.00	0.961
10	Train 1	49.1	1407	Upwards	0.6 to 1.7	5.07	0.959
11	Car	11.5	140	Downwards	0.9 to 1.7	0.51	0.036
12	Car	11.0	140	Downwards	1.1 to 1.8	0.48	0.036

*The pressure measured after the initial pressurisation of the release pipework.

3.2 Blowdown

The mass decay during the tests is based upon measurements of pressure in the storage vessel. As shown in Table 5, the repeated tests for each scenario are relatively consistent. The initial pressure decline in the tank pressure is steeper than once the flow becomes established as the flexible hoses between the storage tank and release point become pressurised. This has resulted in lower initial pressures used for mass flow calculations. After this, the pressure loss follows a typical exponential decay curve.

Using the method from section 2.4, the mass vs time calculations for each scenario are shown in Figure 3. The calculated mass based on the pressure measurements and the approximation form equation 3 are shown in Figure 4. The differential of the curve fit gives the mass flow rates for each test. The initial value of this method (ignoring the pressurisation of the pipework) is displayed in Table 5.

The curve fit for the initial 10 seconds of the release fits well with the calculated mass based on the pressure measurements, which lends credibility to the mass flow values. However, a value of uncertainty has not been established for these values since this is a calculation and approximation rather than a direct measurement.

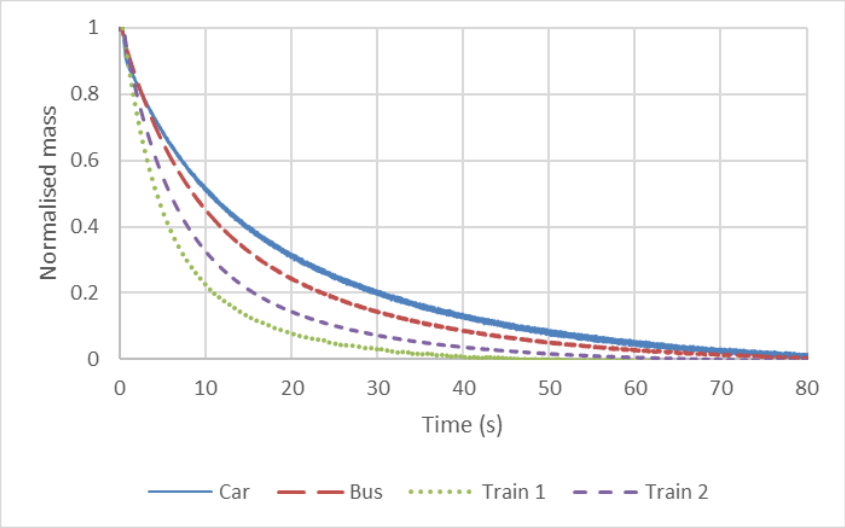

Figure 3: Calculated mass over time for a selection of representative tests

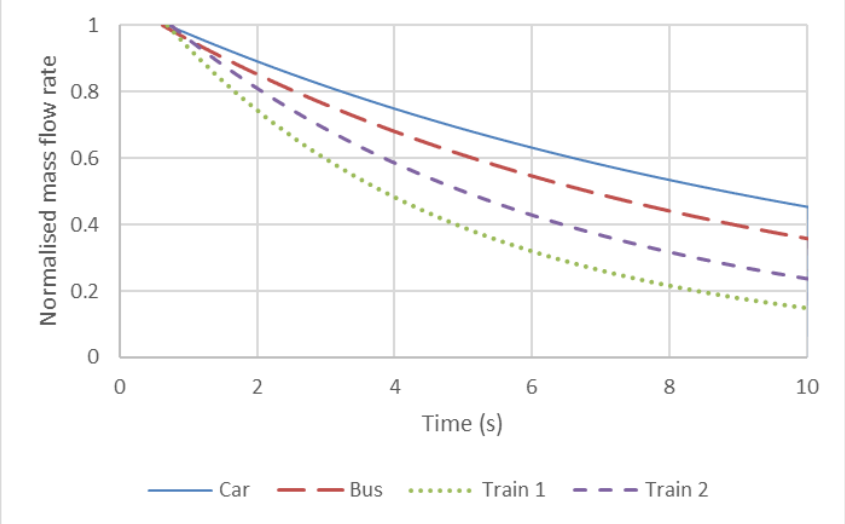

Figure 4: The mass calculated with pressure measurements and the best-fit estimate

Table 6 shows a comparison between the measured mass flow rates at various points for a selection of tests and the predictions made with the E-Labs suite of hydrogen modelling tools [9] assuming a discharge coefficient (C_D) of 1. The measured mass flow rates should be lower that the predicted vales as a real nozzle is used, so by dividing the measured mass flow rate by the E-Labs prediction at various points on the blowdown the effective C_D of the test can be established. This should be less than 1 and near the C_D expected for a nozzle with smooth internal tapering.

Table 6: The equivalent discharge coefficient at three points for various tests.

	t1 (sec)	t2 (sec)	m1 (kg)	m2 (kg)	time point (sec)	Pressure at time point (MPa)	dm/dt meas. at time point (kg/s)	dm/dt e-lab at time point (kg/s)	C_D
Test 4	0	15	3.36	1.08	4.1	20.84	0.152	0.16357	**0.929**
	0	15	3.08	1.45	7.8	15.23	0.10867	0.119	**0.913**
	10	25	1.92	1.12	18.4	7.35	0.05333	0.06178	**0.863**
Test 5	0	15	3.33	1.1	5	19.09	0.14867	0.1544	**0.963**
	0	15	3.1	1.41	8	14.90	0.11267	0.12396	**0.909**
	10	25	1.88	1.06	18	7.40	0.05467	0.06423	**0.851**
Test 6	0	12.25	5.26	0.9	3	35.56	0.35592	0.3641	**0.978**
	0	14	4.4	1.75	8.2	18.10	0.18929	0.21117	**0.896**
	10	25	2.28	1.13	18.2	7.30	0.07667	0.08902	**0.861**
Test 7	0	12	5.44	1	3	35.68	0.37	0.37165	**0.996**
	0	14	4.55	1.8	8.2	18.25	0.19643	0.21781	**0.902**
	10	25	2.4	1.18	18.2	7.44	0.08133	0.09338	**0.871**
Test 8	0	8.6	5.17	1	2	35.31	0.48488	0.49574	**0.978**
	0	12	4.45	0.96	5.5	17.88	0.29083	0.29477	**0.987**
	10	25	1.78	0.54	15.2	5.17	0.08267	0.09305	**0.888**
Test 9	0	8.9	4.9	1	2.5	30.98	0.4382	0.45209	**0.969**
	0	12	4.35	0.88	5.3	18.23	0.28917	0.29844	**0.969**
	10	25	1.7	0.47	15.2	2.22	0.082	0.09088	**0.902**

As can be seen, the C_D values are quite high, particularly initially, and reduce over time. The nozzles have smooth internal tapering, but the results do suggest that the physical system was imperfect. While this could be indicative of the natural variability in experiments with similar initial conditions, an alternate leak path could have developed. During commissioning, the system was capped and integrity checked at the test pressures, which showed that the system held pressure. However, the cap was removed, and the nozzles installed. It is impossible to integrity check a nozzle, so it is possible that the joint of the nozzle introduced an undetected leak path only identifiable during the tests. This would result in higher mass flow rates measured than expected, therefore higher C_D values. This is a feature of real systems, so it is potentially reasonable to assume a C_D of 1 and no friction loss to obtain a worst-case hydrogen cloud for consequence prediction if welded joints are not used.

3.3 Dispersion

The dispersion data was obtained from the hydrogen concentration measurements made throughout the tunnel at 15 points. The purpose of the dispersion measurements was to assess the hydrogen distribution in the following ways: vertical stratification in the cloud, peak hydrogen concentration, and hydrogen cloud propagation down the tunnel.

The peak hydrogen concentrations measured at each point showed little deviation from the mean peak hydrogen concentration throughout the tunnel. This includes no consistent observed vertical stratification, which is demonstrated in Figure 5. The normalised H2 concentration for each test is

shown form the vertical arrays at 5 m and 15 m. Where a sensor reads zero for a test, this has been removed from the mean calculations and attributed to a temporary fault in the sampling system.

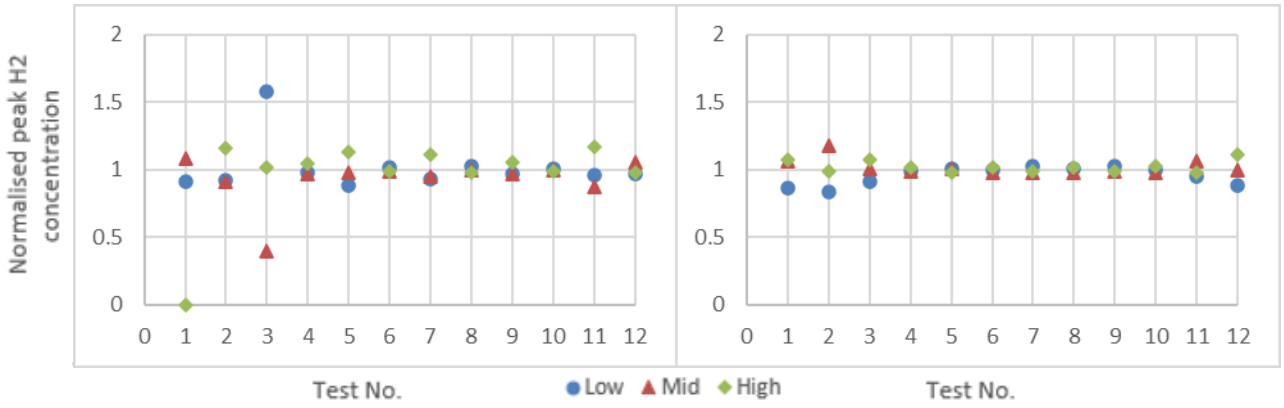

Figure 5: The normalised peak hydrogen concentration for each test at 5 m (left) and 15 m (right).

Figure 6 shows the normalised peak H2 concentration for the 2.5 m position. The low sensor at 2.5 m position consistently measured approximately double the concentration at that location. Comparisons with CFD predictions [5], as well as assessment of the sensor suggest that this sensor was at fault. Measurements made by this sensor were removed from the calculations but are shown to demonstrate the behaviour.

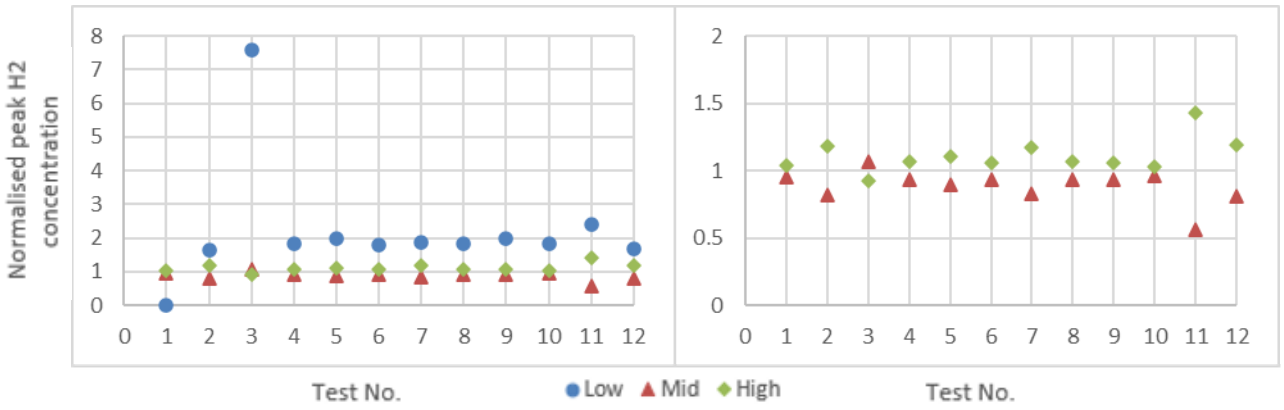

Figure 6: The normalised peak hydrogen concentration for each test at 2.5 m with results from the low sensor (left) and without the low sensor (right).

The car tests (1, 2, 3, 11, 12) showed slightly higher variation in concentration when normalised, however this is due to the proportionally larger effect of small absolute differences when the mean is low. For the results at 2.5 m, the H2 concentration at 3.25 m height was typically higher than that at 2.15 m, but the effect is not significant.

The lack of stratification suggests that the hydrogen mixes effectively and turbulently close to the release point, which was likely encouraged by the orientation of the releases. The releases were all vertical, pointed directly at the tunnel ceiling or floor. This impingement could encourage thorough mixing in the near-field. Horizontal, unimpinged releases could result in different outcomes with more vertical stratification.

The highest measurement point at 3.25 m does leave some space that is not measured at the ceiling where a higher concentration could occur. With the relative homogeneity of the cloud between 0.95 and 3.25 m, a steep gradient between 3.25 and 3.7 m is unlikely but cannot be dismissed based on these experiments.

Table 7 shows the average peak hydrogen concentration measured in the tunnel for each scenario, separated by the wind speed. Increasing the (nominal) wind speed from 1.25 m/s to 2.4 m/s significantly reduces the peak measured concentration measured throughout the tunnel, which demonstrates the dilution effect that tunnel ventilation has. The reductions are significant, reducing the peak hydrogen between 21% to 37% of the low wind speed concentrations. This has the potential to dilute some clouds below the flammable limits, or away from a stoichiometric mix.

Table 7: The effect of ventilation wind speeds on hydrogen dilution.

Scenario	**Average maximum measured concentration -1.25 m/s (% H_2)**	**Average maximum measured concentration – 2.4 m/s (% H_2)**	**Average absolute H_2 reduction (% H_2)**	**Average reduction in concentration (% rd.)**
Car	3.5	2.2	1.3	37
Bus	11	8.7	2.3	21
Train 1	24.4	16.9	7.5	31
Train 2	22.2	14.5	7.7	35

The raw output of the hydrogen sensors is a time series for each measurement point throughout the tunnel. Figure 7 and Figure 8 show the time series for the upper measurement points in the tunnel (3.25 m) to demonstrate the propagation of the hydrogen down the tunnel. The train 1 scenario was selected as the highest mass flow rates and hydrogen concentrations. Test 8 and test 9 are displayed to demonstrate the effect of the ventilation rate not only on the dilution, but also the progression of the hydrogen in the tunnel. The outputs have been aligned based on the expected delay times from the sampling process. The difference in hydrogen cloud propagation can be seen from the graphs as an average 2.5 m/s for the low wind speed, and 4.4 m/s for the high. This suggests that, as well as dilution, increased ventilation rates reduce the residence time of the hazard in the tunnel.

By reviewing the outputs of these sensors, the general behaviour of the release can be surmised. It appears that, as the hydrogen is released, the turbulence of the mixes the gas with the ambient air in the region close to the release point. By 2.5 m lengthwise along the tunnel, the hydrogen has formed a semi-uniform cloud. This is shown by the similar concentrations at various heights in the same lengthwise position. This cloud then travels down the tunnel with limited dilution. The cloud could be pictured as a cylindrical plug with the concentration profile shown in the graphs.

The experiments did not demonstrate the development of stratified flow - as lighter gas from the release progressively intrudes above the tunnel air flow ahead. However, this will probably develop from the observed well mixed “plug” flow further along a tunnel. This is particularly likely to be the structure in the far-field for low wind speeds where interfacial mixing would be suppressed.

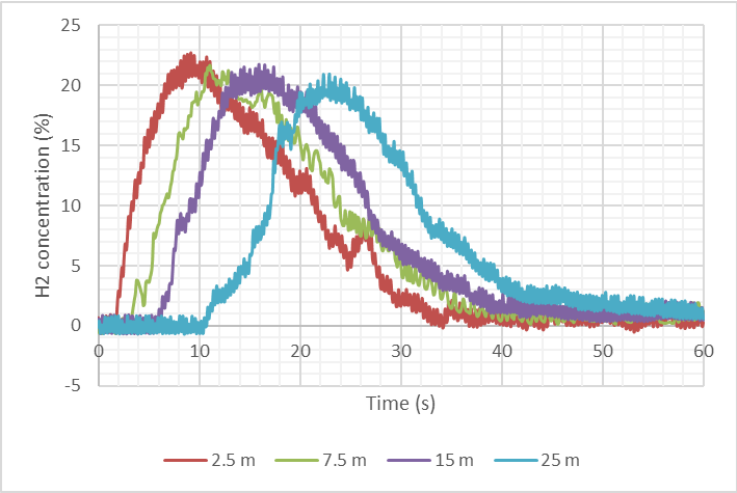

Figure 7: Hydrogen concentration along the tunnel with 1.25 m/s nominal wind speed

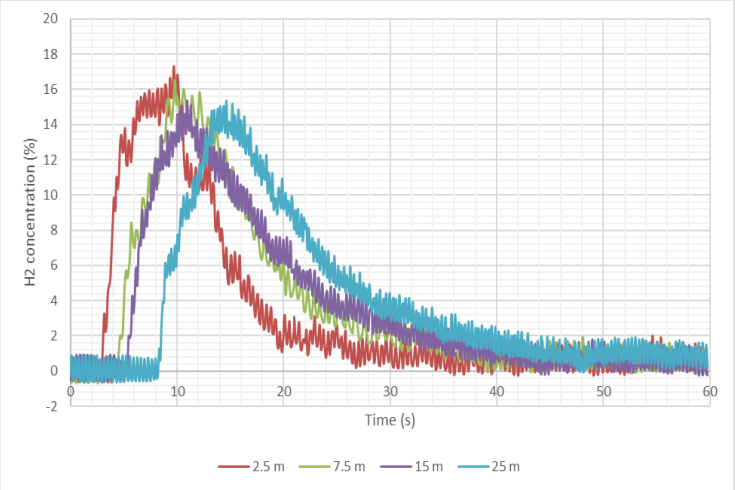

Figure 8: Hydrogen concentration along the tunnel with 2.4 m/s nominal wind speed

4.0 ANALYSIS

4.1 Concentration Correlation

The experimental observations show the formation of a semi-uniform cloud following the blowdown release. To estimate the maximum concentration in this cloud, a correlation between the theoretical fully mixed limit and the measured maximum concentration has been established. The theoretical fully mixed limit is the minimum concentration possible assuming the hydrogen fully mixes with the air flowing down the tunnel in the blowdown time. The equation for the Fully Mixed Limit (FML) is shown in equation 5.

$$FML = \frac{V_{H2}}{V_{H2}+uAt} \times 100 \qquad (5)$$

Where V_{H2} is 90% of the volume of hydrogen at standard pressure released in the blowdown, u is the ventilation rate, A is the area of the tunnel, and t is the time to blowdown 90% of the hydrogen inventory.

The measured maximum hydrogen concentration at any point in the tunnel has a linear correlation with the fully mixed limit in the form show in equation 6 and displayed graphically in Figure 9.

$$C_{H2\ MAX} \approx \frac{1}{E} FML + x \quad (6)$$

Where $C_{H2\ MAX}$ is the peak hydrogen concentration, E is the mixing efficiency factor, taken as 0.95 and x is a constant of 4. Increasing the x constant would ensure a conservative estimate of the maximum concentration in the cloud.

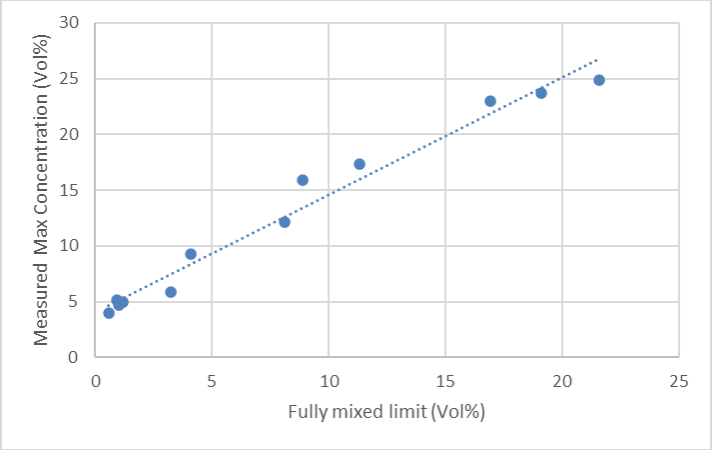

Figure 9: Measured maximum hydrogen concentrations and theoretical fully mixed limit for each test

4.2 Application of Scaling

The scaling methodology was originally based on buoyancy assumptions. The results indicate that the flow that develops from the releases was momentum-dominant then well mixed across the length of the test tunnel. This is due to the core principle that the experiments were scaled based on the idea that the concentration of hydrogen at a proportional height of the tunnel will be similar for a full-scale tunnel. The results show little stratification, so the scaling is less useful than if the cloud had been more buoyancy driven and resulted in stratification.

The scaled initial conditions derived by applying the scaling factors is shown in Table 8. With these initial conditions, in theory, the hydrogen concentrations at relative heights in full-scale tunnels hold. These heights are displayed in Table 9.

Table 8: Scaled extrapolations for each test based on initial conditions and results.

Test No.	Scenario	Scaled release height (m)	Scaled wind speed (m/s)	Scaled initial mass (kg)	Scaled initial mass flow rate (kg/s)
1	Car	0.31	0.75	6.12	0.26
2	Car	0.31	1.89	6.01	0.27
3	Car	0.31	3.62	6.01	0.28
4	Bus	3.2	1.89	39.56	2.39
5	Bus	3.2	3.62	40.39	2.49
6	Train 2	3.7	2.04	100.32	7.88
7	Train 2	3.7	3.92	105.05	8.71
8	Train 1	3.7	2.04	95.39	10.98
9	Train 1	3.7	3.92	94.64	11.14
10	Train 1	3.7	2.04	95.96	11.12
11	Car	0.32	1.89	6.01	0.28
12	Car	0.32	1.89	5.65	0.28

Table 9: Equivalent sensor heights for realistic tunnels.

Sensor height (m)	Road tunnel (8.12 m Ø) equivalent (m)	Train tunnel (9.51 m Ø) equivalent (m)
0.5	1.14	1.33
1.7	3.87	4.53
2.8	6.37	7.46

These masses are similar to those initially envisioned: car: 5.4 kg, bus: 40 kg, train 1: 96 kg, and train 2: 105 kg [2] [8]. Based on the scaling, a 95 kg blowdown with an initial flow rate of 10 kg/s directed vertically upwards at 3.7 m high in a 9.51 m tall tunnel would generate a semi uniform hydrogen cloud in the tunnel between the heights of 1.3 m and 7.5 m. The profile of this cloud would be similar to those displayed in figures 4 and 5. The ventilation rates would be 2 m/s (low) and 3.9 m/s (high).

While the intention is that this scaling would hold, the extrapolation goes beyond the experimental conditions so might not represent full-scale TPRD releases.

5.0 CONCLUSION

In order to investigate the behaviour of hydrogen during a spurious TPRD operation, 12 blowdowns with varying initial conditions were conducted. These experiments were scaled based on the size of the HSE tunnel for both a road and rail tunnel, which resulted in a set of initial conditions representative of these cases.

The mass flow rates, calculated based on pressure and temperature measurements, showed reasonable agreement with those predicted for similar blowdowns. The measured mass flow rate was, however, slightly higher than expected, displayed in high C_D values. This has been attributed to leak paths developing around the nozzle at high pressures, which results in the potential use of a C_D of 1 for a conservative estimate of a blowdown when welded joints are not in use.

The dispersion measurements worked well, however uncertainty in the relative times of the sensors is unavoidable with this setup. This is estimated to be +/- 3 seconds. The observations from these sensors suggest that the blowdown results in rapid mixing near to the release point, forming a semi-uniform cloud with limited vertical stratification that then proceeds down the tunnel with limited dilution down the 25 m of measurements. The dilution, mixing, and stratification could change as the length of the tunnel increases due to buoyancy effects.

Higher ventilation rates increased dilution in all cases, which was observed in the reduced peak concentration measured at each point for the similar initial conditions. A more rapid progression of the hydrogen cloud down the tunnel was also encouraged. The increased ventilation rate therefore reduces both the severity and duration of the hazard.

A correlation was identified based on parameters that could be known prior to an incident occurring. The correlation includes the fully mixed limit, an efficiency factor and a constant and results in a simple method to predict the maximum hydrogen concentration of a blowdown. The results are limited to the initial conditions included in the experiments and may not apply to other scenarios.

The application of the scaling factors was also demonstrated, which shows that the masses of hydrogen in each scenario closely matches the intended value. In theory this enables the concentrations at normalised heights to be used for various tunnel dimensions, however the initial scaling intention was based on buoyancy effects so may have limited use given the observations of hydrogen mixing in the near-field. In particular smaller releases, taller tunnels, or wind speeds outside of those included in the experimental series might not result in the formation of a semi-uniform cloud of hydrogen.

ACKNOWLEDGEMENTS

This project has received funding from the Fuel Cells and Hydrogen 2 Joint Undertaking (now Clean Hydrogen Partnership) under Grant Agreement No. 826193. The contents, including any opinions and/or conclusions expressed, are those of the authors alone and do not necessarily reflect HSE policy.

REFERENCES

1. HyTunnel, “About HyTunnel-CS”, hytunnel.net. https://hytunnel.net/?page_id=31 (accessed Mar. 2023)
2. M. Pursell, M. Garcia, V. Molkov, T Van Esbroeck, and K. Vågsæther, “Report on selection and prioritisation of scenarios”, HyTunnel-CS, Rep. D1.3, 2019.
3. W. Rattigan *et al.* "Results of the deferred experimental programme and associated activities", HyTunnel-CS, Rep. D4.4, 2022.
4. S.G. Giannissi *et al.* “Final report on analytical, numerical and experimental studies on hydrogen dispersion in tunnels, including innovative prevention and mitigation strategies”, HyTunnel-CS, Rep. D2.3, 2022.
5. S.G. Giannissi *et al.*, “CFD dispersion simulations of compressed hydrogen releases through TPRD inside scaled tunnel”, *Int. Conf. Hydrogen Safety*, 2023. – In preparation.
6. W. Buttner, J.E. Hall, S. Coldrick, and T. Wischmeyer, “Hydrogen wide area monitoring of LH2 repelases”, *Int. J. Hydrogen Energy*, 46 (2021): 12497 – 12510,
7. D.J. Hall and S. Walker. “Scaling rules for reduced-scale field releases of hydrogen fluoride.” *J. Hazardous Materials*, 54 (1997): 89-111.
8. S.G. Giannissi *et al.* “Intermediate report on analytical, numerical and experimental studies”, HyTunnel-CS, Rep. D2.2, 2020.
9. E-laboratory. (2020). FCH2 education. FCH2 Education. https://fch2edu.eu/home/e-laboratory/
10. I.A. Johnston, “The Nobel-Abel equation of state: Thermodynamic derivations for ballistics modelling”, Australian DoD, DSTO, DSTO-TN-0670, 2005.